Nov 10th, 12:00 AM - 12:00 AM

Finite Element Modeling of Concrete Shrinkage in Composite Deck Slabs

Vitaliy V. Degtyarev

Wei-Wen Yu International Specialty Conference on Cold-Formed Steel Structures
Baltimore, Maryland, U.S.A, November 9 & 10, 2016

Finite Element Modeling of Concrete Shrinkage in Composite Deck Slabs

Vitaliy V. Degtyarev[1]

Abstract

This paper presents finite element models of composite deck slabs subjected to restrained concrete shrinkage. The models created in ANSYS and validated against test data were based on the assumption of the full shear interaction between the deck and the concrete and accounted for concrete creep, cracking, and nonlinear stress-strain relationship. Concrete shrinkage was modeled by temperature changes applied to concrete. The effects of different shrinkage profiles, concrete creep, and deck slab properties on the long-term concrete and deck strains are presented. Future research work is outlined.

Introduction

It is well known that concrete shrinkage may negatively affect flexural stiffness of reinforced concrete and composite members when they are restrained against volume change (Bradford 2010, Gilbert 1999, Lamport and Porter 1990, and Scanlon and Bischoff 2008). Therefore, the effects of concrete shrinkage on the long-term deflection of reinforced concrete and composite members should be taken into consideration in the design to obtain reliable estimates of the actual deflections.

Relatively little research has been reported on the shrinkage induced stresses and deformations of composite deck slabs. Recent experimental studies have revealed a non-uniform shrinkage distribution through the slab thickness due to the impermeable steel deck at the slab soffit (Al-deen and Ranzi 2015, Gholamhoseini 2014, and Gilbert et al. 2012). The non-uniform shrinkage profile resulted in reduced concrete tensile stress in the concrete bottom fiber and, in uncracked slabs, in an increased shrinkage induced curvature of the cross-section when compared with the uniform shrinkage profile observed in reinforced concrete members exposed on both sides (Gilbert et al. 2012).

[1] Design Engineer, New Millennium Building Systems, Columbia, SC, USA

Bradford (2010) proposed an analytical model for the description of the service load behavior of composite slabs that accounts for the non-uniform shrinkage profile and the partial interaction between the deck and the concrete. Gilbert et al. (2012) extended an analytical method presented by Gilbert and Ranzi (2010) to the time-depended analysis of composite deck slabs with the non-uniform shrinkage distribution and the full shear interaction between the deck and the concrete. Although the developed analytical models give an engineer a tool to account for the effects of shrinkage on the long-term behavior of composite slabs, they are based on simplified assumptions, which may or may not apply to real composite slabs. The Bradford (2010) model assumes uncracked concrete and linear stress-strain relationships at the deck-concrete interface, whereas the Gilbert et al. (2012) model assumes elastic instantaneous concrete deformations and the full interaction between the deck and the concrete.

Modern standards for the design of composite deck slabs provide no guidance on accounting for concrete shrinkage in slab deflection calculations. This may be due to the fact that the composite slabs have traditionally been used over relatively short spans, where the slab design was not controlled by the deflection. In recent years, relatively thin long-spanning composite slabs, which design is often controlled by the deflection, have been gaining popularity. Therefore, the effects of concrete shrinkage on the composite slab stiffness and the behavior shall be extensively studied to allow for the development of simple and reliable design provisions.

Experimental studies are obviously the most preferable source of information about long-term behavior of engineering structures. They, however, are expensive and time consuming. The finite element (FE) analysis may supplement the experimental studies and help to reduce the number of tests. It may also provide information about stress and strain distributions in the deck and the concrete that may not be easily obtained from the experiments.

There is a limited number of published papers related to modeling concrete shrinkage in FE analysis. Attiyah et al. (2014) and Ma and Gao (2008) modeled concrete shrinkage in ANSYS by converting shrinkage strains into equivalent temperature strains. A temperature change resulting in the required temperature strain was applied to each concrete node of the model. The temperature change was calculated using the coefficient of thermal expansion of concrete.

The objectives of this study were to develop FE models of composite deck slabs capable of accounting for the effects of concrete shrinkage on the long-term strains in the slabs and to perform a preliminary parametric study. The effects of the shrinkage strain profile, concrete creep, deck height and

thickness, concrete cover, and welded wire fabric on the long-term strains in the slabs due to concrete shrinkage were considered in the parametric study. The FE models were developed in ANSYS.

Numerical study program

The numerical study described in this paper was performed in three phases. In phase one, FE models were developed and validated using available test data. In phase two, the effects of different shrinkage profiles on the long-term strains in the deck and the concrete were studied. The phase three consisted of a parametric study where the effects of deck slab properties on the long-term strains in the slabs were investigated.

Finite element model development and validation

Two nonlinear three-dimensional FE models of composite deck slabs formed on Fielders KF40 and KF70 trapezoidal profiles tested by Gholamhoseini (2014) were developed in this phase. The KF40 and KF70 profiles were 1.57 in. (40 mm) and 2.76 in. (70 mm) deep, respectively. Both profiles were 0.0295 in. (0.75 mm) thick. The total slab depth of both profiles was 5.9 in. (150 mm). Fig. 1 shows cross sections of the modeled slabs. WWF was not used in the tests and in the models. The KF40 and KF70 deck slab models were square in plan with side lengths of 29.29 in. (744 mm) and 24.41 in. (620 mm), respectively.

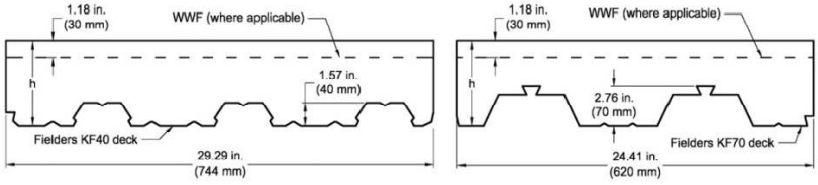

Fig 1. Modeled composite slabs

The concrete was modeled with eight-node 3D reinforced concrete solid elements SOLID65, which are capable of plastic deformations, cracking in tension, and crushing in compression. The multilinear isotropic hardening plasticity (MISO) of concrete in compression was combined with the William-Warnke failure criterion (William and Warnke, 1975) in tension to model the nonlinear material behavior of concrete. The uniaxial stress-strain relationships for concrete in compression were obtained using the Desayi and Krishnan model (Desayi and Krishnan 1964) not accounting for the descending branch of the curve: $f_c = (E_c\varepsilon_c)/(1 + (\varepsilon_c/\varepsilon_0)^2)$, where f_c is stress at any strain ε_c; $\varepsilon_0=2f'_c/E_c$ is strain at the concrete compressive strength f'_c; and E_c is concrete

initial tangent modulus. The concrete compressive strength, the concrete initial tangent modulus, and the concrete ultimate uniaxial tensile strength used in the models were 5,004 psi (34.5 MPa), 4293117 psi (29600 MPa), and 508 psi (3.5 MPa), respectively – the same as those in the tests (Gilbert et al. 2012). The shear transfer coefficients of 0.3 and 1.0 were specified for open and closed cracks, respectively. The concrete was assumed to have a Poisson's ratio of 0.2.

Each slab was modeled either accounting for or not accounting for concrete creep. The ANSYS primary explicit creep equation for C6=0 was used to describe the creep behavior of the SOLID65 elements: $\dot{\varepsilon}_{cr} = C_1 \sigma^{C_2} \varepsilon_{cr}^{C_3} e^{-C_4/T}$, where $\dot{\varepsilon}_{cr}$ is change in equivalent strain with respect to time; σ is equivalent stress; T is temperature; and C_1 to C_4 are constants. The following values of the constants were used in the models: C_1=4.869×10^{-5}, C_2=1, C_3=-0.974, and C_4=0, which were determined by equating the explicit creep equation to the creep equation given in *fib* (2010) and taking the actual slab properties and relative humidity during testing into consideration.

The steel deck was modeled with 4-node structural shell elements SHELL181. The bilinear isotropic hardening material model (BISO) using von Mises plasticity was specified for the deck. The deck was assumed to be elastic-perfectly plastic. An elastic modulus of 29008 ksi (2.00×10^5 MPa) and a Poisson's ratio of 0.3 were used for the deck.

The deck and the concrete were discretized with quadrilateral and hexahedral meshes, respectively (Fig. 2), and had common nodes at the contact surfaces, which represented the full shear interaction between the deck and the concrete. A line of the concrete nodes at approximately one-fourth of the slab length from the slab end was restricted from translations in the directions parallel and perpendicular to the deck span (see Fig. 2). Another line of the concrete nodes at approximately one-fourth of the slab length from another slab end was restricted from translations in the directions perpendicular to the deck span. Translations of two concrete nodes at the top of the slab at approximately one-fourth of the slab length from both ends were restrained in the direction perpendicular to the slab plane.

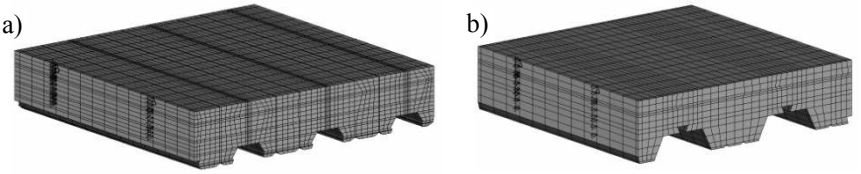

Fig. 2. FE models of analyzed slabs: a) KF40 deck slab; b) KF70 deck slab

The concrete shrinkage behavior was modeled in the same way as it was done by Attiyah et al. (2014) and Ma and Gao (2008). Temperature changes were applied to each concrete node. The temperature changes were determined so that the resulting temperature strain equals to the free shrinkage strain measured on concrete specimens without deck as follows: $\Delta T = \varepsilon_{sh}/\alpha_c$, where $\varepsilon_{sh}$is the free shrinkage strain; α_c is the coefficient of thermal expansion of concrete (6.67×10^{-6} /°F [12×10^{-6} /°C]). The non-uniform free shrinkage strain profiles experimentally obtained by Gholamhoseini (2014) were used. The temperature changes applied to concrete nodes varied through the slab depth. The sparse direct equation solver and the automatic load stepping were used in the analyses. The L2 norm (square root sum of the squares) of force and moment with tolerance values of 0.05 and 0.005, respectively were specified.

Fig. 3 shows distributions of total strains in the slab models due to the concrete shrinkage obtained from the FE analyses and from tests (Gholamhoseini 2014). The total strains include shrinkage strains and mechanical strains, as well as creep strains (where applicable) developed with time due to the restrained shrinkage. Fig. 3 shows that the developed FE models predicted the strain distributions and the curvatures of the tested slabs reasonably well considering the large variability in shrinkage measurements (Gilbert et al. 2012).

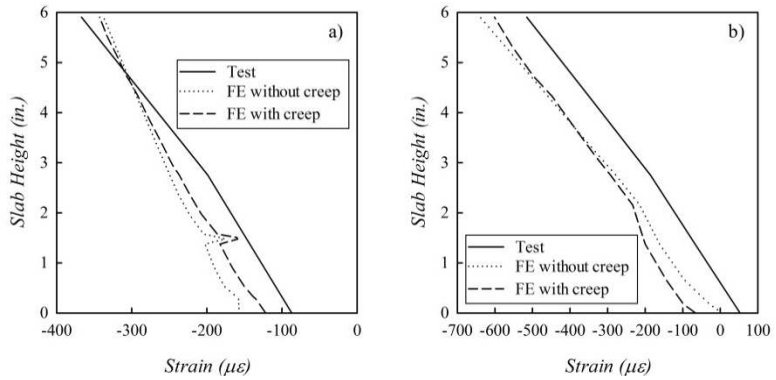

Fig. 3. Total strain distributions a) KF40 deck slabs and b) KF70 deck slabs

The concrete creep affected the strain distributions and the curvatures of the KF40 and KF70 deck slabs differently. In the KF40 deck slabs, the creep resulted in larger concrete strains and cross-section curvature, whereas in the KF70 deck slabs, the effect of the creep was the opposite. Concrete crack distributions in the FE models shown in Fig. 4 explain the difference.

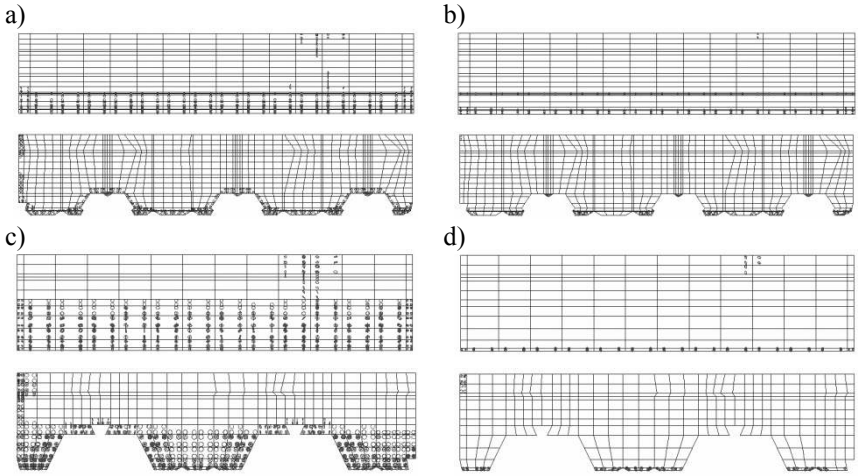

Fig. 4. Cracks in FE models a) and b) KF40 deck slabs without and with creep, respectively; c) and d) KF70 deck slabs without and with creep, respectively

Both models demonstrated less extensive concrete cracking when the concrete creep was taken into consideration, which is explained by concrete stress relaxation due to the creep. However, the difference in the crack development was relatively small for the KF40 deck slabs and significant for the KF70 deck slabs. Due to the more extensive cracking, the flexural stiffness of the KF70 deck slabs without the creep was reduced when compared with the slabs with the creep, which resulted in larger strains and cross-section curvature of the KF70 deck slabs without the creep.

Effects of different shrinkage strain profiles

Effects of different shrinkage strain profiles on the long-term strains in the deck and the concrete were studied on the KF70 deck slab models. Four different shrinkage strain profiles were considered: uniform, triangular, bilinear, and parabolic (Fig. 5). The shrinkage strain profiles were exactly the same as those considered by Gilbert et al. (2012) in their parametric study. For each strain profile, two analyses were performed: with and without taking concrete creep into consideration. Fig. 6 shows concrete and deck strains induced by different shrinkage strain profiles. The concrete slab portions with the mechanical tensile strains larger than 124×10^{-6} were cracked. The mechanical concrete tensile strains larger than 124×10^{-6} included cracking strains.

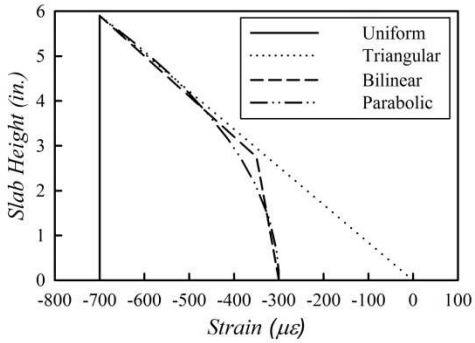

Fig. 5. Shrinkage strain profiles considered in parametric study

The uniform shrinkage profile resulted in the highest mechanical concrete compressive and tensile strains when compared with other considered profiles. Due to the higher concrete tensile strains and more extensive cracking, the curvature of the model with the uniform shrinkage distribution was the highest among all considered shrinkage profiles. Accounting for the concrete creep in the model with the uniform shrinkage profile resulted in noticeably higher mechanical concrete top strains and slightly smaller bottom strains. The curvature of the model that accounted for the creep was slightly greater when compared with the model that did not account for the creep. The uniform shrinkage distribution resulted in the highest deck bottom flange strains and the smallest deck top flange strains when compared with the other shrinkage strain profiles. The concrete creep resulted in increased deck top flange strains and reduced deck bottom flange strains.

The triangular shrinkage strain profile resulted in very small mechanical concrete strains. In contrast to the model with the uniform shrinkage distribution, the top of the slab was in tension. The slab model curvature for the triangular shrinkage strain profile was smaller than that for the uniform shrinkage but larger than that for the bilinear and parabolic shrinkage strain distributions. The concrete creep resulted in slightly larger mechanical concrete strains and slightly smaller curvature. Deck bottom strains were relatively small. They slightly increased when the concrete creep was considered in the model.

The bilinear and parabolic shrinkage distributions resulted in comparable mechanical concrete bottom strains, which were larger than those for the triangular but smaller than those for the uniform distributions.

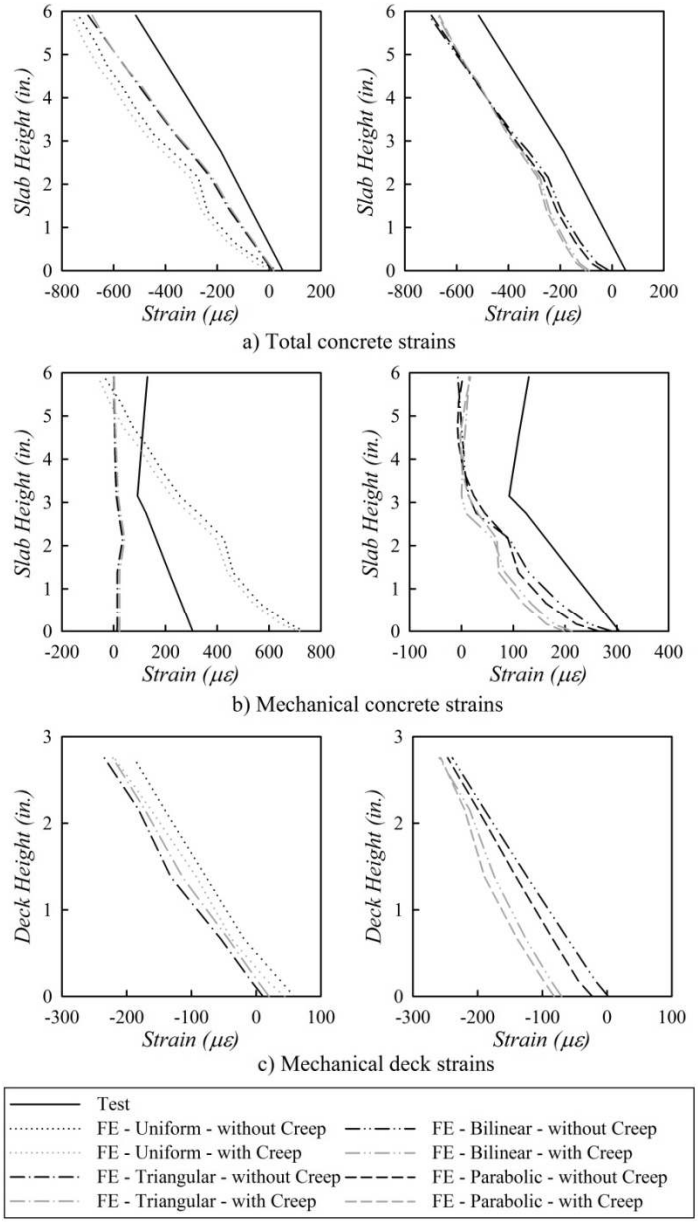

Fig. 6. Concrete and deck strains induced by different shrinkage strain profiles

With the creep, the slab top was in tension for both shrinkage profiles. The curvatures were comparable and slightly smaller than those for the uniform and triangular distributions especially when the creep was considered. The concrete creep resulted in smaller curvatures, smaller mechanical concrete strains at the bottom, larger concrete tensile strains at the top, and higher deck compressive strains. The entire deck section was in compression for both distributions when the creep was considered and for the parabolic profile without the creep.

The bilinear and parabolic shrinkage strain profiles are the ones that most accurately represent the measured shrinkage distributions in composite deck slabs. They also result in better predictions of total and mechanical concrete strains when compared with the uniform and triangular shrinkage profiles. Therefore, any of these two profiles can be used in the numerical studies.

Effects of composite deck slab properties

The effects of the deck height and thickness, concrete topping thickness, and the amount of temperature and shrinkage reinforcement on the long-term deck and concrete strains due concrete shrinkage were studied. The composite deck slab models consisted of either KF40 or KF70 decks, which were either 0.0295 in. (0.75 mm) or 0.0591 in. (1.5 mm) thick, and normal weight concrete topping of either 3.15 in. (80 mm) or 4.33 in. (110 mm) thick. The slab models were assumed to contain no temperature and shrinkage reinforcement or to be reinforced with SL82 (0.30 in. [7.6 mm] diameter at 7.87 in. [200 mm] on center spacing) or SL81 (0.30 in. [7.6 mm] diameter at 3.94 in. [100 mm] on center spacing) wire mesh. Twenty four slab models were analyzed. The parabolic shrinkage profile with the strains of -700×10^{-6} and -300×10^{-6} at the slab top and bottom, respectively, were used in the models. These shrinkage strains were assumed to be developed after 322 days of drying. The concrete creep was accounted for in the FE models.

Figs. 7, 8, and 9 show total concrete strains, mechanical concrete strains, and mechanical deck strains in the analyzed slab models. Fig. 8 demonstrates that in all analyzed models the concrete cracked at the slab bottom due to the restrained shrinkage. The wire mesh provided another restraint for the concrete shrinkage, which resulted in an increased concrete tension at the WWF level and at the top of the slabs. In all analyzed KF70 deck slab models, the concrete cracked at the WWF level due to the restrained shrinkage, which shows that WWF may cause concrete cracking.

The effect of the deck height on the mechanical concrete top strains depended on the concrete and deck thickness and the WWF amount. The slab top was in compression in the 0.0591 in. (1.5 mm) thick deck slabs without WWF.

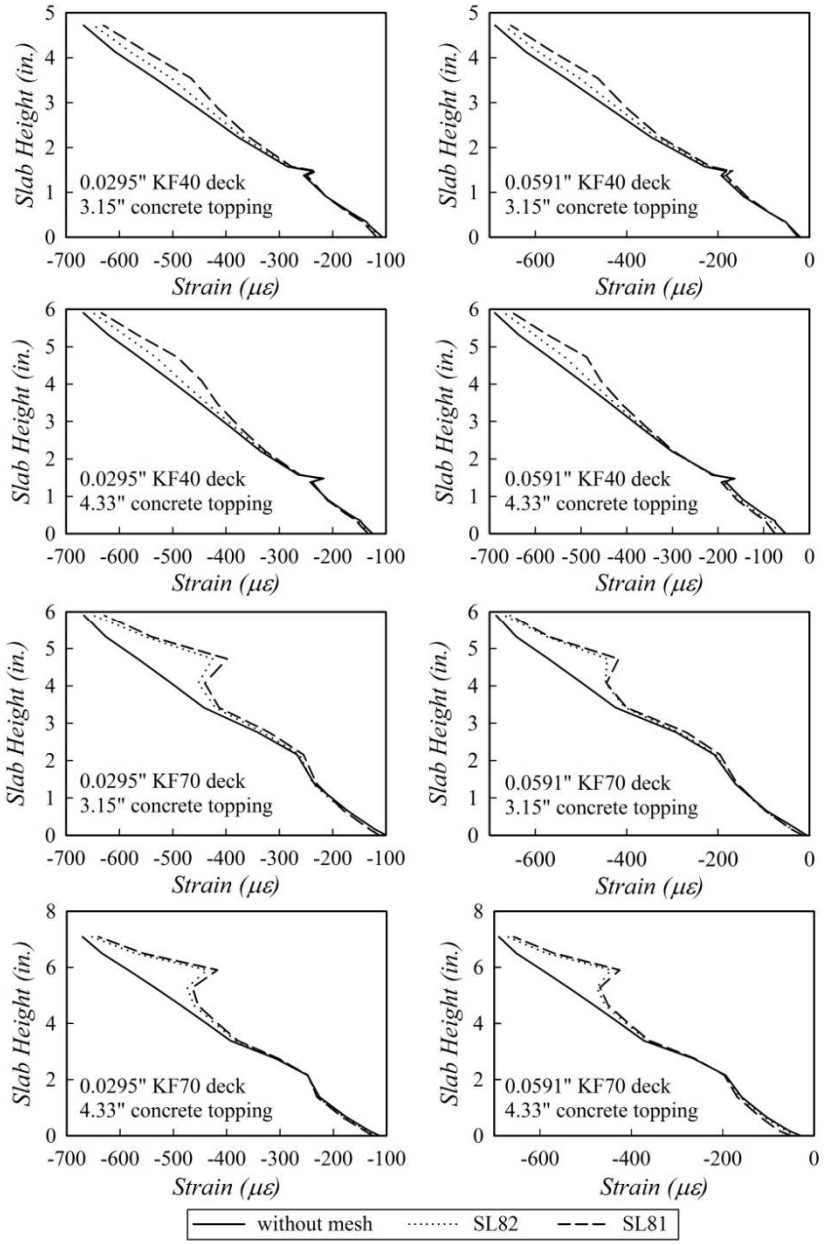

Fig. 7. Total concrete strains in analyzed deck slab models

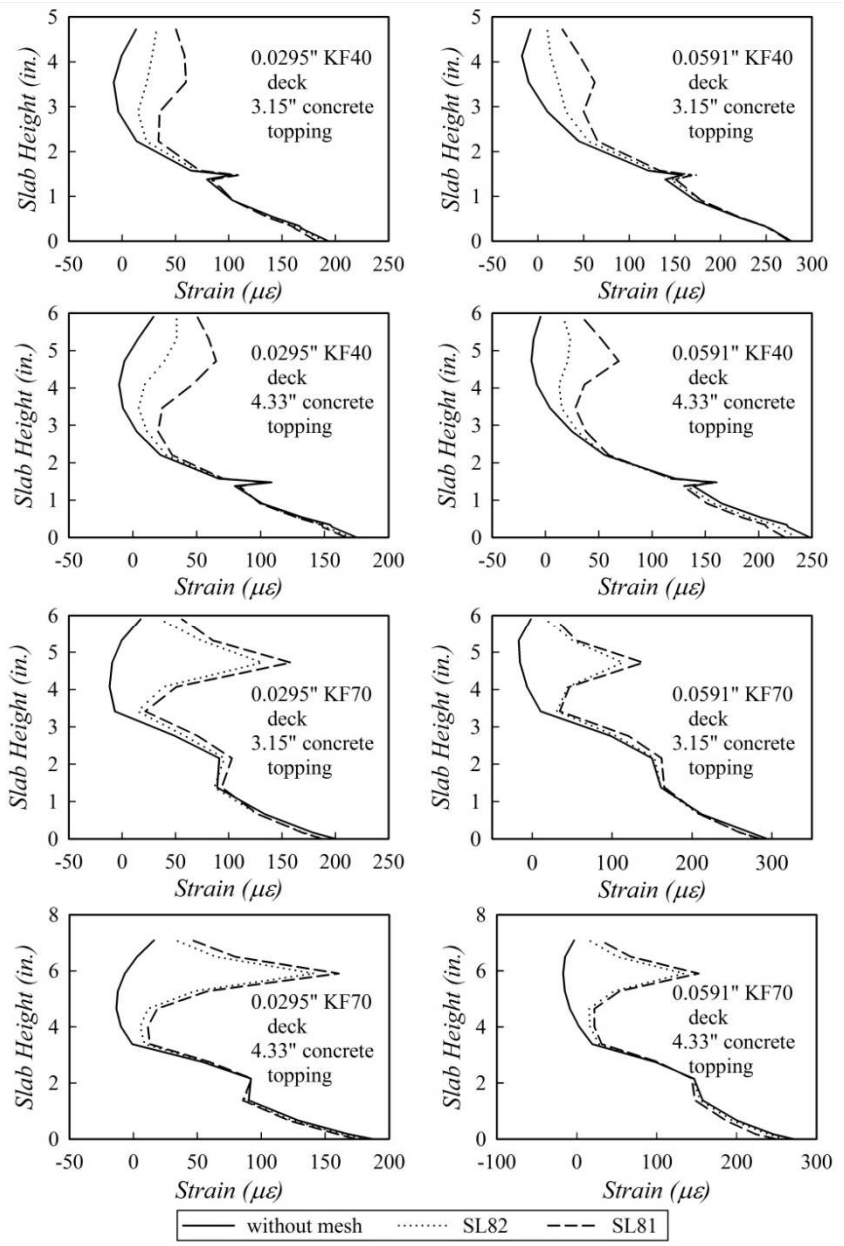

Fig. 8. Mechanical concrete strains in analyzed deck slab models

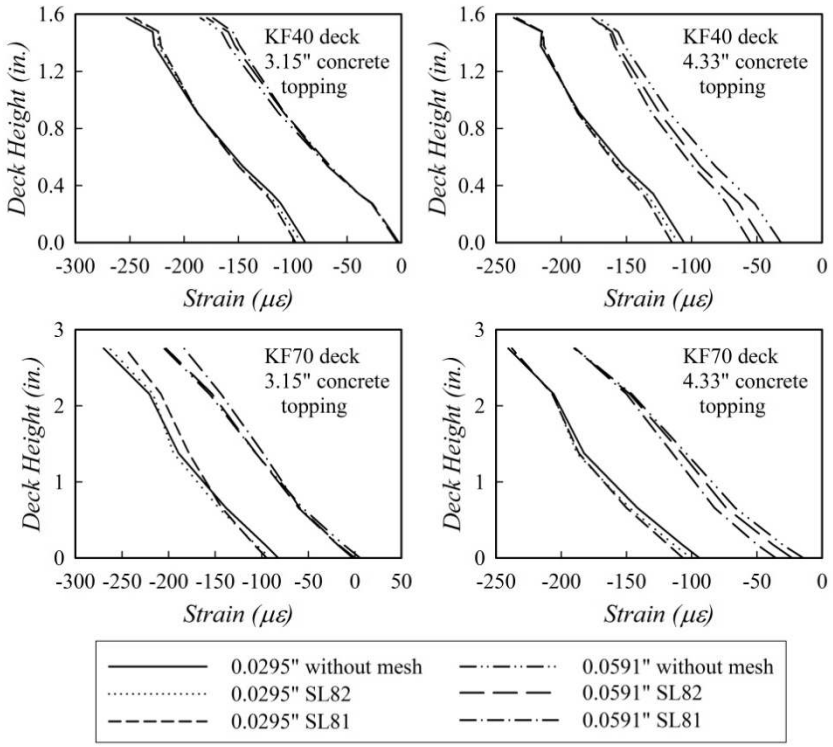

Fig. 9. Mechanical deck strains in analyzed deck slab models

In those slabs, the mechanical concrete compressive strains at the slab top reduced when the deck height increased. The top of all other analyzed models was in tension. In those models, the mechanical concrete top strains increased and decreased for the slabs with the concrete cover of 3.15 in. (80 mm) and 4.33 in. (110 mm), respectively, when the deck height increased. An increase in the deck thickness resulted in reduced mechanical concrete tensile strains at the slab top.

An increase in the concrete cover resulted in reduced and increased mechanical concrete compressive top strains in the 0.0591 in. (1.5 mm) thick KF40 and KF70 deck slab models, respectively. In all other models, which top was in tension, the mechanical concrete tensile top strains either did not change or slightly increased for the KF40 deck slabs and either did not change or slightly decreased for the KF70 deck slabs. The mechanical concrete tensile strains at the top of the slab and at the WWF level increased as the WWF area increased.

The mechanical concrete strains at the WWF level significantly increased when the deck height increased for all considered models. In the KF40 deck slabs, the mechanical concrete strains at the WWF level did not exceed the ultimate concrete tensile strain, while in the KF70 deck slabs, the concrete cracked at the WWF level in all analyzed models. No definitive effect of the deck thickness on the mechanical concrete strains at the WWF level was found for the KF40 deck slabs. For the analyzed KF70 deck models, the mechanical concrete tensile strains at the WWF level decreased when the deck thickness increased. The concrete cover above the deck practically did not affect the mechanical concrete strains at the WWF level in the KF40 deck slabs with the SL82 mesh. In the KF40 deck slabs with the SL81 mesh and in the KF70 deck slabs with the SL82 and SL81 meshes, the mechanical concrete tensile strains at the WWF level increased when the concrete cover thickness increased.

The mechanical concrete strains at the bottom of the models increased when the deck height and thickness increased and decreased when the concrete cover and the WWF area increased. The mechanical compressive strains in the deck bottom flange increased when the concrete cover and the WWF area are increased and reduced when the deck height and thickness increased.

The mechanical compressive strains in the deck top flange increased when the deck height increased and reduced when the deck thickness and the WWF area increased. When the concrete cover increased, the mechanical compressive strains in the deck top flange decreased in the slab models with the 0.0591 in. (1.5 mm) thick KF40 and KF70 decks reinforced with the SL81 mesh and increased in all other slab models.

The slab curvature increased when the deck thickness increased and reduced when the deck height, the concrete topping thickness, and the WWF area increased. This indicates that the composite deck slab deflection induced by the concrete shrinkage will be larger in the slabs on heavier deck and smaller in the slabs with deeper deck and concrete cover, as well as in the slabs with heavier WWF.

Conclusions and future work

Nonlinear three-dimensional FE models of composite deck slabs capable of accounting for the effects of concrete shrinkage on the long-term strains and deformations in the slabs were developed in this study using the commercial software ANSYS and validated against published test data. The FE models were based on the assumption of the full shear interaction between the deck and the concrete and accounted for concrete creep, cracking, and nonlinear

stress-strain relationship. The concrete shrinkage was modeled by temperature changes applied to concrete.

The effects of different shrinkage profiles, concrete creep, and deck slab properties on the long-term concrete and deck strains were investigated. The study showed that the bilinear and parabolic shrinkage strain distributions, being the most realistic ones, provide a better agreement between concrete strains from the tests and the analysis when compared with the uniform and triangular distributions. The concrete creep may noticeably affect concrete strains and slab curvature induced by the restrained shrinkage. The concrete creep on one hand reduces mechanical concrete tensile strains, which contribute to less extensive concrete cracking and, therefore, greater flexural stiffness of the slab and its smaller curvature. On the other hand, it increases total concrete strains, which contribute to larger slab curvature.

The effects of the deck height and thickness, concrete cover thickness, and the WWF amount on the long-term concrete and deck strains and the slab curvature were studied. In all analyzed slab models, concrete cracked at the slab bottom due to the restrained shrinkage. The wire mesh provided another restraint for the concrete shrinkage, which resulted in an increased concrete tension at the WWF level and at the slab top. The concrete in some analyzed slab models cracked at the WWF level due to the restrained shrinkage. It was shown that the slab curvature increased when deck thickness increased and reduced when the deck height, the concrete cover, and the WWF area increased.

The full shear interaction between the deck and the concrete was used in the developed FE models. In the reality, the composite deck slabs demonstrate partial interaction. Therefore, the effects of the partial interaction on the long-term concrete and deck strains and the slab curvature induced by the restrained concrete shrinkage should be investigated. More extensive parametric studies based on wider ranges of deck types, slab thicknesses, and reinforcing parameters should be performed to develop recommendations for taking concrete shrinkage into consideration in the design of the composite slabs. Considering many uncertainties involved in the concrete shrinkage and the deck and concrete interaction, a probabilistic approach should be used in the design recommendations development.

Acknowledgements

The author thanks South Ural State University and personally to Dr. Natalia Degtyareva for providing access to ANSYS available at the University.

References

Al-deen, S. and Ranzi, G. (2015). "Effects of non-uniform shrinkage on the long-term behaviour of composite steel-concrete slabs." *International Journal of Steel Structures*, 15(2), 415-432.

Attiyah, A.N., Gesund, H., and Rasool, M.H. (2014). "Finite element modeling of concrete shrinkage cracking in walls." *Kufa Journal of Engineering*, 5(1), 127-140.

Bradford, M.A. (2010). "Generic modelling of composite steel–concrete slabs subjected to shrinkage, creep and thermal strains including partial interaction." *Engineering Structures*, 32(5), 1459–1465.

Bradford, M.A., Gilbert, R.I., Zeuner, R., and Brock, G. (2011). "Shrinkage deformations of composite slabs with open trapezoidal sheeting." *Procedia Engineering*, 14, 52-61.

Desayi, P., and Krishnan, S. (1964). "Equation for the stress-strain curve of concrete." *Journal of the American Concrete Institute*, 61(3), 345-350.

fib. (2010). *Model Code 2010. First Complete Draft. Volume 1*, fédération internationale du béton, Lausanne, Switzerland.

Gholamhoseini, A. (2014). "Time-dependent behaviour of composite concrete slabs," Ph.D. Thesis, The University of New South Wales, Sydney, Australia.

Gholamhoseini, A., Gilbert, R.I., Bradford, M., and Chang, Z.-T. (2014). "Time-dependent deflection of composite concrete slabs." *ACI Structural Journal*, 111(4), 765-775.

Gilbert, R.I. (1999). "Deflection calculation for reinforced concrete structures—why we sometimes get it wrong." *ACI Structural Journal*, 96(6), 1027-1032.

Gilbert, R.I., Bradford, M.A., Gholamhoseini, A., and Chang, Z.-T. (2012). "Effects of shrinkage on the long-term stresses and deformations of composite concrete slabs." *Engineering Structures*, 40, 9-19.

Gilbert, R.I. and Ranzi, G. (2010). Time-depended behaviour of concrete structures. London: Spon Press, 426p.

Lamport, W.B. and Porter, M.L. (1990). "Deflection predictions for concrete slabs reinforced with steel decking." *ACI Structural Journal*, 87(5), 564-571.

Ma, B.G. and Gao, Y.L. (2008). "Finite element analysis for shrinkage in the interface of functionally graded concrete segment used in shield tunneling." Key Laboratory for Silicate Materials Science and Engineering of Ministry of Education, Wuhan University of Technology, Wuhan, China, 430070.

Ranzi, G., Leoni, G., and Zandonini, R. (2013). "State of the art on the time-dependent behaviour of composite steel-concrete structures." *Journal of Constructional Steel Research*, 80, 252-263.

Scanlon, A. and Bischoff, P.H. (2008). "Shrinkage restraint and loading history effects on deflections of flexural members." *ACI Structural Journal*, 105(4), 498-506.

Willam, K. J., and Warnke, E. D. (1975). "Constitutive model for the triaxial behavior of concrete." *Proc., International Association for Bridge and Structural Engineering,* 19, 1-30.